Clonal Vγ6$^+$Vδ4$^+$ T cells promote IL-17–mediated immunity against *Staphylococcus aureus* skin infection

Mark C. Marchitto[a], Carly A. Dillen[a], Haiyun Liu[a], Robert J. Miller[a], Nathan K. Archer[a], Roger V. Ortines[a], Martin P. Alphonse[a], Alina I. Marusina[b], Alexander A. Merleev[b], Yu Wang[a], Bret L. Pinsker[a], Angel S. Byrd[a], Isabelle D. Brown[a], Advaitaa Ravipati[a], Emily Zhang[a], Shuting S. Cai[a], Nathachit Limjunyawong[c,d], Xinzhong Dong[c,d,e], Michael R. Yeaman[f,g,h,i], Scott I. Simon[j], Wei Shen[k], Scott K. Durum[k], Rebecca L. O'Brien[l,m], Emanual Maverakis[b], and Lloyd S. Miller[a,n,o,p,1]

[a]Department of Dermatology, Johns Hopkins University School of Medicine, Baltimore, MD 21231; [b]Department of Dermatology, School of Medicine, University of California, Davis, Sacramento, CA 95817; [c]The Solomon H. Snyder Department of Neuroscience, Johns Hopkins University School of Medicine, Baltimore, MD 21205; [d]The Center for Sensory Biology, Johns Hopkins University School of Medicine, Baltimore, MD 21205; [e]Howard Hughes Medical Institute, Johns Hopkins University School of Medicine, Baltimore, MD 21205; [f]Division of Molecular Medicine, Harbor–UCLA Medical Center, Torrance, CA 90502; [g]Division of Infectious Diseases, Harbor–UCLA Medical Center, Torrance, CA 90502; [h]Department of Medicine, David Geffen School of Medicine at UCLA, Los Angeles, CA 90095; [i]Los Angeles Biomedical Research Institute, Harbor–UCLA Medical Center, Torrance, CA 90502; [j]Department of Biomedical Engineering, University of California, Davis, CA 95616; [k]Cytokines and Immunity Section, Cancer and Inflammation Program, Center for Cancer Research, National Cancer Institute, National Institutes of Health, Bethesda, MD 20892; [l]Department of Biomedical Research, National Jewish Health, Denver, CO 80206; [m]Department of Immunology and Microbiology, University of Colorado Health Sciences Center, Aurora, CO 80206; [n]Department of Medicine, Division of Infectious Diseases, Johns Hopkins University School of Medicine, Baltimore, MD 21287; [o]Department of Orthopaedic Surgery, Johns Hopkins University School of Medicine, Baltimore, MD 21287; and [p]Department of Materials Science and Engineering, Johns Hopkins University, Baltimore, MD 21218

Edited by Rino Rappuoli, GlaxoSmithKline, Siena, Italy, and approved April 18, 2019 (received for review October 31, 2018)

T cell cytokines contribute to immunity against *Staphylococcus aureus*, but the predominant T cell subsets involved are unclear. In an *S. aureus* skin infection mouse model, we found that the IL-17 response was mediated by γδ T cells, which trafficked from lymph nodes to the infected skin to induce neutrophil recruitment, proinflammatory cytokines IL-1α, IL-1β, and TNF, and host defense peptides. RNA-seq for *TRG* and *TRD* sequences in lymph nodes and skin revealed a single clonotypic expansion of the encoded complementarity-determining region 3 amino acid sequence, which could be generated by canonical nucleotide sequences of *TRGV5* or *TRGV6* and *TRDV4*. However, only *TRGV6* and *TRDV4* but not *TRGV5* sequences expanded. Finally, Vγ6$^+$ T cells were a predominant γδ T cell subset that produced IL-17A as well as IL-22, TNF, and IFNγ, indicating a broad and substantial role for clonal Vγ6$^+$Vδ4$^+$ T cells in immunity against *S. aureus* skin infections.

Staphylococcus aureus | IL-17 | T cells | neutrophils | skin

The gram-positive extracellular bacterium *Staphylococcus aureus* causes the vast majority of skin infections in humans (1). In addition, *S. aureus* has become increasingly resistant to antibiotics, and multidrug-resistant community-acquired methicillin-resistant *S. aureus* (CA-MRSA) strains cause severe skin and invasive infections (e.g., cellulitis, pneumonia, bacteremia, endocarditis, osteomyelitis, and sepsis) in otherwise healthy individuals outside of hospitals, creating a serious public health concern (2, 3).

If immune-based therapies are to provide an alternative to antibiotics, an increased understanding of protective immunity against *S. aureus* skin infections is essential. This is imperative, because all prior *S. aureus* vaccines targeting antibody-mediated phagocytosis failed in human clinical trials (4). Notably, an *S. aureus* vaccine targeting the surface component iron surface determinant B against deep sternal wound infections and bacteremia following cardiothoracic surgery had a worse outcome, as individuals who suffered an *S. aureus* infection were five times more likely to die if they had received the vaccine rather than placebo (5).

As an alternative to antibody responses, there has been a recent focus on T cells in contributing to protective immunity against *S. aureus* infections. In humans, a variety of T cell subsets and cytokines has been implicated in host defense against *S. aureus*. For example, rare genetic diseases characterized by reduced IL-17–producing CD4$^+$ T cells (i.e., Th17 cells) or IL-17–mediated immune responses (e.g., autosomal dominant hyper-IgE syndrome, IL-17F deficiency, and IL-17RA receptor deficiency) have an increased susceptibility to *S. aureus* skin infections (6–9). Similarly, in mouse models, IL-17 produced by γδ T cells and/or Th17 cells was found to be important in neutrophil recruitment and host defense against *S. aureus* skin and bacteremia infections (10–16). However, in vaccination attempts in mouse models of *S. aureus* skin

Significance

Staphylococcus aureus is the most common cause of skin infections and is becoming increasingly resistant to antibiotics. If immune-based therapies are to provide an alternative to antibiotics, a better understanding of immunity to *S. aureus* skin infections is crucial. During an *S. aureus* skin infection in mice, a clonal Vγ6$^+$Vδ4$^+$ T cell population expressing a single complementarity-determining 3 (CDR3) region encoded by canonical *TRGV6* and *TRDV4* sequences expanded in the skin-draining lymph nodes, trafficked to infected skin, and promoted IL-17–mediated immune clearance by inducing neutrophil recruitment, inflammatory cytokines, and host defense peptides. Together, identification of a clonal T cell population in immunity to *S. aureus* skin infections provides a specific response to target for future vaccines and immunotherapies.

Author contributions: M.C.M., C.A.D., H.L., N.K.A., M.P.A., A.I.M., A.A.M., A.S.B., N.L., X.D., M.R.Y., S.I.S., W.S., S.K.D., R.L.O., E.M., and L.S.M. designed research; M.C.M., C.A.D., H.L., R.J.M., N.K.A., R.V.O., M.P.A., A.I.M., A.A.M., Y.W., B.L.P., A.S.B., I.D.B., A.R., E.Z., S.S.C., N.L., and W.S. performed research; A.I.M., A.A.M., W.S., S.K.D., R.L.O., and E.M. contributed new reagents/analytic tools; M.C.M., C.A.D., H.L., R.J.M., N.K.A., R.V.O., M.P.A., A.I.M., A.A.M., Y.W., B.L.P., A.S.B., I.D.B., A.R., E.Z., S.S.C., N.L., X.D., M.R.Y., S.I.S., W.S., S.K.D., R.L.O., E.M., and L.S.M. analyzed data; and M.C.M., C.A.D., H.L., N.K.A., A.I.M., A.A.M., M.R.Y., S.I.S., S.K.D., R.L.O., E.M., and L.S.M. wrote the paper.

Conflict of interest statement: M.R.Y. is a cofounder of NovaDigm Therapeutics, which is developing novel vaccines and immunotherapeutics for infectious diseases, including *S. aureus*. L.S.M. has received grant support for work unrelated to the work reported in this manuscript from AstraZeneca, Pfizer, Regeneron Pharmaceuticals, Moderna Therapeutics, and Boehringer Ingelheim, is on the scientific advisory board for Integrated Biotherapeutics, and is a shareholder of Noveome Biotherapeutics, which are each developing vaccines and therapeutics against *S. aureus* and other pathogens.

This article is a PNAS Direct Submission.

Data deposition: The RNA-sequencing data reported in this paper have been deposited in the NCBI Sequence Read Archive (SRA) (accession no. SRP194263).

[1]To whom correspondence may be addressed. Email: lloydmiller@jhmi.edu.

This article contains supporting information online at www.pnas.org/lookup/suppl/doi:10.1073/pnas.1818256116/-/DCSupplemental.

Published online May 14, 2019.

and bacteremia infection, the IL-17–mediated protection was thought to be mediated by Th17 cells rather than γδ T cells (17–20). Additionally, IFNγ-producing $CD4^+$ T cells (Th1 cells) were found to contribute to protection against *S. aureus* skin infections in patients with HIV disease as well as in *S. aureus* wound and bacteremia infections in mouse models (21–23). Another study found that the IFNγ produced by human $CD8^+$ T cells contributed to antigen-induced immunity against *S. aureus* (24). We previously reported that IFNγ and TNF protected against a recurrent *S. aureus* skin infection in mice deficient in IL-1β (25). Finally, several studies have reported that IL-22 contributes to host defense peptide production and bacterial clearance of an *S. aureus* skin infection or mucosal colonization (10, 26–28).

Taken together, these findings in humans and mice suggest that different T cell subsets and their cytokine responses are involved in immunity against *S. aureus* infections. However, whether a predominant T cell subset and effector cytokine responses contribute to host defense against *S. aureus* skin infections is unclear. In particular, the studies in humans and mice suggest an important role for IL-17 responses in immunity against *S. aureus*, but the precise T cell sources and ensuing immune responses are not entirely understood. Therefore, we chose to determine the specific T cell subsets and mechanisms of IL-17–mediated immunity in cutaneous host defense in an in vivo mouse model of an *S. aureus* skin infection.

Results

Recruited Lymphocytes from Lymph Nodes Are Required for IL-17–Mediated Host Defense. First, to determine whether the protective T cell immune response against an *S. aureus* skin infection was mediated by T cells residing in the skin or T cells recruited from lymph nodes, an intradermal (i.d.) *S. aureus* infection model was used (11, 25, 29–31) in which the bioluminescent CA-MRSA USA300 LAC::*lux* strain was injected intradermally into the back skin of mice ± FTY720 (administered on days −1, 0, and 1, and every other day thereafter until day 14 postinfection), which inhibits lymphocyte egress (including all T cells) from lymph nodes (25, 32). We chose to investigate the role of IL-17A and IL-17F because they are produced by many different T cell subsets and have been implicated in a variety of mouse models of *S. aureus* infection as being critical to host defense (10–16). For these experiments, we used an IL-17A-tdTomato/IL-17F-GFP dual-color reporter mouse strain, which is on a C57BL/6 background and produces normal levels of IL-17A and IL-17F. Before performing in vivo experiments, this reporter mouse strain was validated in vitro by culturing $CD3^+$ T cells from skin-draining lymph nodes of IL-17A-tdTomato/IL-17F-GFP dual-color reporter mice in the presence of Th17/IL-17 polarizing conditions. We found that the expression of tdTomato and GFP by Th17 cells and γδ T cells closely corresponded to the expression of endogenous IL-17A and IL-17F protein levels using specific mAbs and intracellular flow cytometry (*SI Appendix*, *Methods* and Fig. S1).

Using this reporter mouse strain, we found that FTY720 treatment resulted in significantly increased skin lesion sizes and in vivo bioluminescence imaging (BLI) signals [which highly correlates with ex vivo CFUs harvested at different time points after the *S. aureus* i.d. skin infection (11, 25, 33)], compared with no treatment ($P < 0.05$) (Fig. 1 *A* and *B*). In vivo whole-animal fluorescence imaging (FLI) was sequentially employed (following in vivo BLI) to evaluate IL-17A expression (tdTomato fluorescence) and IL-17F expression (GFP fluorescence) in the *S. aureus*-infected skin in the anesthetized mice noninvasively over time. The in vivo FLI signals for tdTomato (IL-17A) and GFP (IL-17F) that peaked on day 7 were completely inhibited by treatment with FTY720 ($P < 0.001$) (Fig. 1 *C* and *D*). In addition, skin biopsy specimens of the *S. aureus*-infected skin obtained on day 7 were also evaluated by immunofluorescence microscopy for tdTomato-labeled IL-17A–producing cells and GFP-labeled IL-17F–producing cells, and these fluorescently labeled cells were found interspersed within the inflammatory infiltrate in the dermis

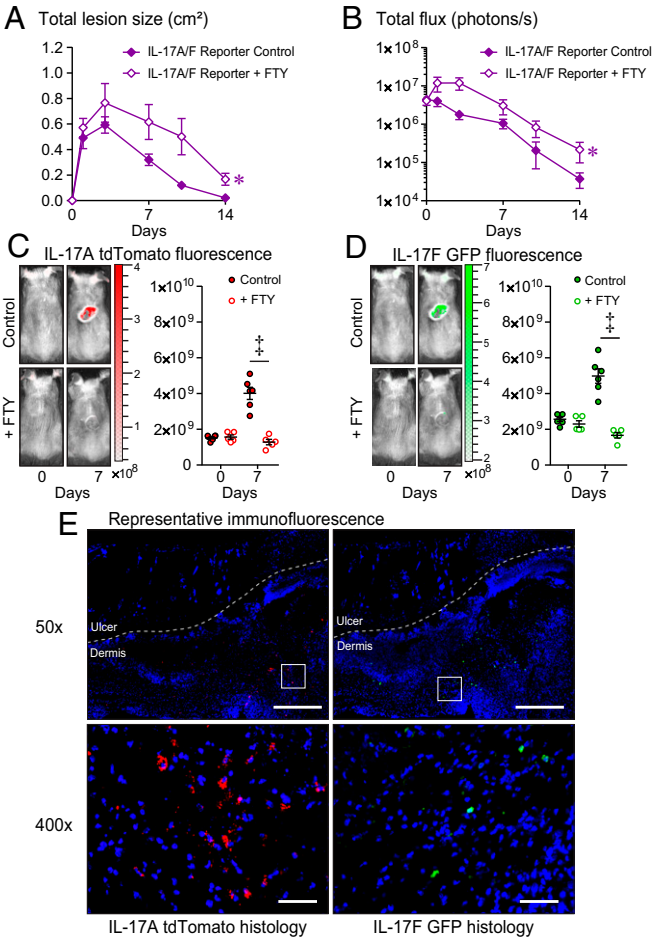

Fig. 1. Recruitment of IL-17A/F–producing T cells from lymph nodes to the skin is required for host defense against *S. aureus* skin infection. *S. aureus* skin infection was performed on IL-17A-tdTomato/IL-17F-GFP dual-color reporter mice (IL-17A/F reporter) ± FTY720 treatment (n = 5–10 mice per group). (*A*) Mean total lesion size (cm^2) ± SEM. (*B*) Mean total flux (photons/s) ± SEM. (*C* and *D*) Representative in vivo fluorescence imaging signals and mean tdTomato (IL-17A) (*C*) or GFP (IL-17F) (*D*) total radiant efficiency ([p/s]/[μW/cm^2]) ± SEM. (*E*) *S. aureus*-infected skin was harvested on day 7, and immunofluorescence microscopy labeling with anti-tdTomato and anti-GFP mAbs demonstrating localization of IL-17A/F production within cells in the dermis. [Scale bars, 500 μm (50×) and 50 μm (400×).] $^*P < 0.05$, $^‡P < 0.001$, as calculated by a two-way ANOVA (*A* and *B*) or two-tailed Student's t test (*C* and *D*). Data are representative of two independent experiments.

underlying the necrotic epidermis and upper dermis (Fig. 1*E*). Taken together, IL-17A/F–producing cells that mediated host defense against the *S. aureus* skin infection in vivo were recruited from lymph nodes to the *S. aureus*-infected skin, and inhibition of this trafficking resulted in worsening of the infection.

γδ T Cells Are the Major Cellular Source of IL-17. Next, to determine the T cell subset that produced the IL-17A and IL-17F, lymph nodes and skin samples from wild-type (wt) C57BL/6 mice were obtained on days 0 (naïve), 3, 7, and 14 during the *S. aureus* skin infection, and intracellular labeling for $IL\text{-}17A^+$–, $IL\text{-}17F^+$–, and $IL\text{-}17A/F^+$–producing cells was performed and quantified by flow cytometry (Fig. 2 *A*–*D*). In the skin-draining lymph nodes, there were statistically greater total numbers of γδ T cells and $CD4^+$ T cells on days 3 and 7, compared with naïve mice (day 0) ($P < 0.001$) (Fig. 2*A*). In addition, in the lymph nodes there were markedly increased numbers of $IL\text{-}17A^+$ and $IL\text{-}17A/F^+$ γδ T cells (which peaked on day 7) and barely detectable numbers of $IL\text{-}17F^+$ γδ T

cells ($P < 0.001$). There were also increased numbers of IL-17A$^+$ CD4$^+$ T cells (which also peaked on day 7) and to a much lesser extent IL-17F$^+$ and IL-17A/F$^+$ CD4$^+$ T cells ($P < 0.001$) (Fig. 2*B*). In addition to differences in cell numbers, the mean fluorescence intensity (MFI) of IL-17A–expressing γδ T cells was fivefold higher than IL-17A–expressing CD4$^+$ T cells, whereas the MFI of IL-17F–expressing CD4$^+$ T cells was slightly higher than IL-17F–expressing γδ T cells (*SI Appendix*, Fig. S2), indicating that γδ T cells produced substantially higher amounts of IL-17A but similar amounts of IL-17F as CD4$^+$ T cells.

In the *S. aureus*-infected skin, there was a statistically greater total number of γδ T cells on days 7 and 14 (which peaked on day 7) ($P < 0.01$) and CD4$^+$ T cells on days 3, 7, and 14 ($P < 0.01$), compared with naïve mice (Fig. 2*C*). In the *S. aureus*-infected skin, there was a substantial increase in the numbers of IL-17A$^+$ γδ T cells (which peaked on day 7) and to a lesser extent IL-17F$^+$ and IL-17A/F$^+$ γδ T cells ($P < 0.05$). In the skin, there was also an increase in the numbers of IL-17F$^+$ CD4$^+$ T cells (which peaked on day 7), which were greater than the slightly increased numbers of IL-17A$^+$ CD4$^+$ T cells ($P < 0.001$), but the numbers of both IL-17A$^+$ and IL-17A/F$^+$ CD4$^+$ T cells remained close to the low background numbers of naïve mice (Fig. 2*D*).

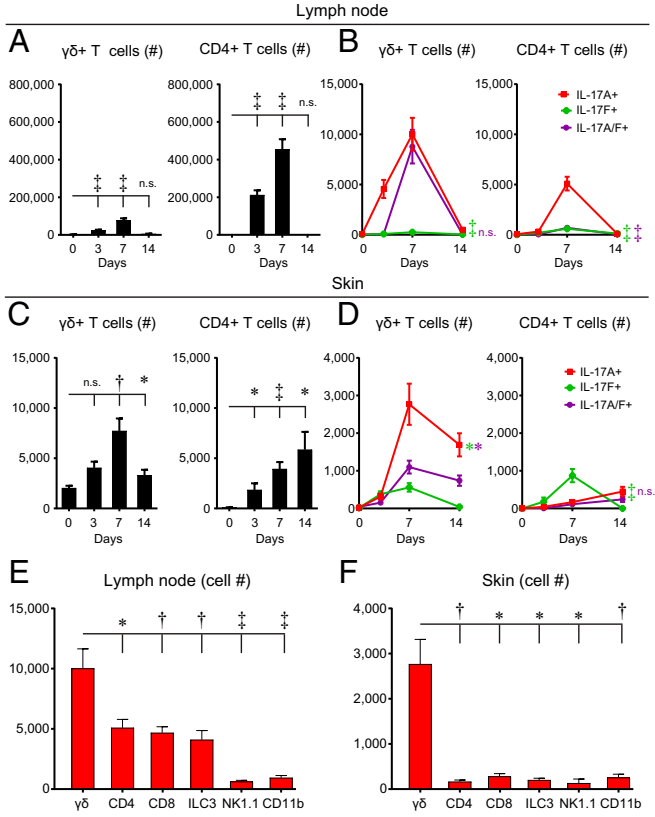

Fig. 2. γδ T cells are a predominant cellular source of IL-17A in the lymph nodes and *S. aureus*-infected skin. Skin-draining lymph nodes and skin specimens were harvested from wt mice on days 0 (naïve), 3, 7, and 14 after *S. aureus* skin infection, and flow cytometry was performed ($n = 10$ per group). (*A* and *C*) Mean number of γδ and CD4$^+$ T cells ± SEM isolated from lymph nodes (*A*) or skin (*C*). (*B* and *D*) Mean number of IL-17A$^+$, IL-17F$^+$, and IL-17A/F$^+$ γδ and CD4$^+$ T cells ± SEM isolated from lymph nodes (*B*) or skin (*D*). (*E* and *F*) Mean cell number ± SEM of IL-17A$^+$ cells, including γδ T cells, CD4$^+$ T cells, CD8$^+$ T cells, ILC3s (CD45$^+$CD127$^+$RORγt$^+$, Lin$^-$), natural killer cells (NK1.1$^+$), and myeloid cells (CD11b$^+$) isolated from skin-draining lymph nodes (*E*) and *S. aureus*-infected skin (*F*) on day 7. $^*P < 0.05$, $^\dagger P < 0.01$, $^\ddagger P < 0.001$, as calculated by a two-tailed Student's *t* test. n.s., not significant. Data are a compilation of two independent experiments.

Next, total lymph node cells from day 7 of the *S. aureus* skin infection were obtained to determine the number of ex vivo IL-17A$^+$ cells after PMA/ionomycin stimulation. γδ T cells represented the most abundant cellular source of IL-17A$^+$, compared with CD4$^+$ T cells, CD8$^+$ T cells, innate lymphoid cells 3 (ILC3s), natural killer (NK) cells, and CD11b$^+$ myeloid cells (Fig. 2*E*). In addition, immune cells from *S. aureus*-infected skin samples were obtained to determine the number of ex vivo IL-17A$^+$ cells after PMA/ionomycin stimulation, especially since myeloid cells can be a source of IL-17A in other models of infection and inflammation (34). We found that γδ T cells were the most abundant cellular source of IL-17A, and there were fewer numbers of IL-17A$^+$ CD11b$^+$ cells and other cell types (Fig. 2*F*). Collectively, these data indicate that γδ T cells were the most abundant cellular source of IL-17 in the skin-draining lymph nodes and *S. aureus*-infected skin.

IL-17A and IL-17F Have Compensatory and Redundant Roles in Host Defense. In other bacterial, fungal, and viral infection models, IL-17A and IL-17F have been shown to have either redundant or differential roles in immune responses (12, 35–37). In particular, Ishigame et al. (12) reported redundant activity of IL-17A and IL-17F in spontaneous *S. aureus* mucocutaneous infections that developed in their mouse colony in mice with constitutive genetic deletion of both IL-17A and IL-17F but not deletion of IL-17A or IL-17F alone. However, 16S rDNA sequencing revealed that *S. aureus* was not present in the skin microbiome of our mouse colony (38), and consequently our IL-17A/F–deficient mice did not spontaneously develop *S. aureus* mucocutaneous infections. This provided the opportunity for us to investigate the relative contribution and temporal dynamics of IL-17A and IL-17F responses that occurred during the course of an acute *S. aureus* skin infection, which would be more representative of how acute *S. aureus* skin infections commonly occur in humans. Therefore, the *S. aureus* i.d. infection model was performed in mice deficient in both IL-17A and IL-17F (IL-17A/F$^{-/-}$) and wt C57BL/6 mice. IL-17A/F$^{-/-}$ mice developed significantly increased lesion sizes during the course of infection that peaked on day 7 compared with wt mice ($P < 0.05$) (*SI Appendix*, Fig. S3 *A* and *B*). In addition, IL-17A/F$^{-/-}$ mice had significantly increased bacterial burden during the course of infection as measured by in vivo BLI, especially from days 3–14 compared with wt mice ($P < 0.01$) (*SI Appendix*, Fig. S3 *C* and *D*). These data were similar to the increased lesion size data and in vivo BLI data observed in FTY720-treated mice (Fig. 1 *A* and *B*), providing further evidence that the IL-17A/F response was due to recruited γδ T cells. To confirm the in vivo BLI data, on day 7 the *S. aureus*-infected skin was homogenized and ex vivo CFUs were enumerated (*SI Appendix*, Fig. S3*E*). IL-17A/F$^{-/-}$ mice had statistically greater (i.e., approximately fourfold) ex vivo CFUs compared with wt mice ($P < 0.01$). Taken together, these results suggest that γδ T cell-derived IL-17A and/or IL-17F contributed to host defense during the *S. aureus* skin infection, especially at time points beyond day 3 after the bacterial skin inoculation.

To further evaluate the contribution of IL-17A versus IL-17F, wt mice were treated systemically (i.p. injection) with an anti–IL-17A neutralizing mAb, an anti–IL-17F neutralizing mAb, anti–IL-17A and anti–IL-17F neutralizing mAbs combined, or an isotype control mAb (*SI Appendix*, Fig. S3 *F* and *G*). Anti–IL-17A and anti–IL-17F neutralizing mAbs combined resulted in statistically increased lesion sizes ($P < 0.001$) and in vivo BLI signals ($P < 0.001$) during the course of infection compared with isotype mAb-treated wt mice. In contrast, there were no significant differences in lesion sizes or in vivo BLI signals with treatment of either anti–IL-17A mAb alone or anti–IL-17F mAb alone compared with isotype mAb-treated wt mice. To further evaluate the contribution of IL-17A versus IL-17F, IL-17A/F$^{-/-}$ mice were administered recombinant IL-17A (rIL-17A) or rIL-17F along with the i.d. bacterial inoculum in the skin (*SI Appendix*, Fig. S3 *H* and *I*). As in *SI Appendix*, Fig. S3 *B* and *D*, IL-17A/F$^{-/-}$ mice had significantly

increased lesion sizes and bacterial burden as measured by in vivo BLI during the course of infection compared with wt mice ($P < 0.001$). However, administration of either rIL-17A or rIL-17F resulted in significantly reduced lesion sizes ($P < 0.001$) and lower in vivo BLI signals ($P < 0.001$ and $P < 0.05$, respectively) (similar to those observed in wt mice) compared with IL-17A/F$^{-/-}$ mice. Taken together, since neutralization of both IL-17A and IL-17F was required to observe an immune defect in wt mice and treatment with either rIL-17A or rIL-17F was sufficient to rescue the immune impairment in IL-17A/F$^{-/-}$ mice, these findings indicate that γδ T cell-derived IL-17A and IL-17F have redundant and compensatory roles in host defense against an *S. aureus* skin infection.

IL-17A/F–Deficient Mice Develop Increased Skin Necrosis and Bacterial Clusters and Impaired Neutrophil Recruitment. Based upon histologic analysis on day 7 after infection, IL-17A/F$^{-/-}$ mice had significantly increased width of epidermal and dermal skin necrosis compared with wt mice ($P < 0.05$) (Fig. 3 *A* and *B*), which is consistent with the larger skin lesion sizes observed by gross morphology using digital photography (Fig. 3 *A* and *B*). In addition, in Gram stain and anti-*S. aureus* lipoteichoic acid (LTA) antibody-labeled sections, IL-17A/F$^{-/-}$ mice had a statistically significant increase in width of the horizontal band of bacterial clusters in the dermis (underlying the area of skin necrosis), compared with wt mice (Fig. 3*A*, white arrowheads and Fig. 3*C*), corroborating the increased bacterial burden as measured by in vivo BLI and ex vivo CFUs in IL-17A/F$^{-/-}$ mice compared with wt mice (*SI Appendix*, Fig. S3 *C–E*).

To evaluate whether the immune impairment in IL-17A/F$^{-/-}$ mice was due to defective neutrophil, monocyte, and/or macrophage recruitment, day 3 and 7 skin biopsies were harvested and the numbers of these myeloid cells were determined by flow cytometry, according to Ly6G^{hi}Ly6C^{int} (neutrophils), Ly6G^{lo}Ly6C^{hi} (monocytes), and CD11b^{+}F4/80^{+} (macrophages) (Fig. 3 *D* and *E*). On day 3, there was no significant difference in neutrophil number between IL-17A/F$^{-/-}$ mice and wt mice. However, on day 7, IL-17A/F$^{-/-}$ mice had nearly a threefold statistically significant reduction in neutrophils compared with wt mice. In addition, IL-17A/F$^{-/-}$ mice also had significantly decreased monocyte numbers on day 3 and macrophage numbers on day 7 compared with wt mice. However, these slight differences in monocyte and macrophage numbers might not be as biologically relevant as the differences in neutrophil numbers, because there were more than ∼15- to 30-fold fewer monocytes and macrophages than neutrophils during the *S. aureus* skin infection.

IL-17A/F–Deficient Mice Express Decreased Proinflammatory Cytokines and Host Defense Peptides. Next, to determine whether IL-17A and IL-17F contributed to expression of other proinflammatory cytokines, day 7 skin biopsies were evaluated for mRNA and protein levels of IL-1α, IL-1β, and TNF, which have each been implicated in immunity against *S. aureus* skin infections (25, 30, 31). IL-17A/F$^{-/-}$ mice had markedly decreased mRNA transcript expression of *IL1A* ($P < 0.001$), *IL1B* ($P < 0.01$), and *TNF* ($P < 0.001$), significantly decreased protein levels of IL-1β ($P < 0.05$) and TNF ($P < 0.05$), and a trend toward decreased protein levels of IL-1α ($P = 0.06$) (Fig. 4 *A* and *B*). As expected, IL-17A was not detected in IL-17A/F$^{-/-}$ mice. In contrast to these findings, there was no difference between mRNA or protein levels of IFNγ in IL-17A/F$^{-/-}$ mice and wt mice.

In addition, several host defense peptides have either bacteriostatic or bactericidal activity against *S. aureus* in various different mouse models of *S. aureus* infection, including psoriasin (S100a7) (10), calprotectin (S100a8/S100a9) (39), β-defensins (mBD3, mBD4, and mBD14) (10, 40, 41), lipocalin 2 (42), cramp (10, 43, 44), Reg3γ (45), and Slurp1 (27), but whether the expression of these relevant host defense peptides is regulated by IL-17A or IL-17F during an in vivo *S. aureus* skin infection is incompletely understood. Therefore, we performed our *S. aureus* skin infection

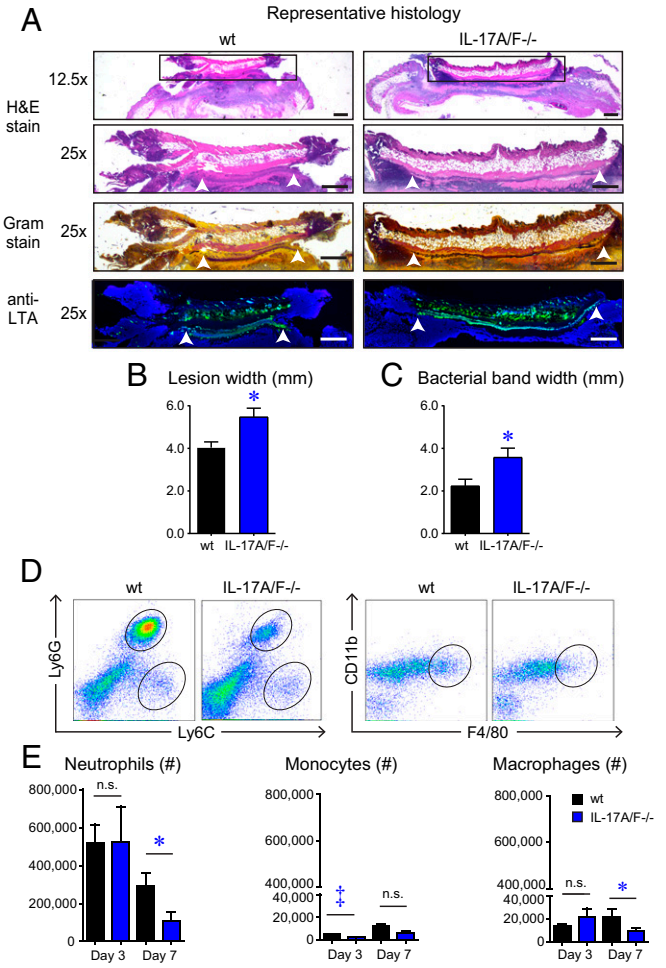

Fig. 3. IL-17A/F–deficient mice develop increased skin necrosis and bacterial burden along with impaired neutrophil recruitment. *S. aureus* skin infection was performed on IL-17A/F$^{-/-}$ and wt mice and the infected skin tissue was harvested on day 7 for histology ($n = 8$ mice per group) and on days 3 and 7 for flow cytometry analysis ($n = 10$ mice per group). (*A*) Representative histology of skin biopsy specimens obtained on day 7 and stained with hematoxylin and eosin (H&E) stain or Gram stain and immunofluorescence labeling with an anti-LTA mAb. The three *Lower* panels (25×) are from the boxed area in the *Upper* panel (12.5×). (Scale bars, 500 μm.) White arrowheads indicate peripheral ends of the horizontal band of bacterial clusters in the dermis. (*B*) Mean skin necrosis width (mm) ± SEM. (*C*) Mean bacterial band width (mm) ± SEM. (*D*) Representative flow plots of neutrophils (Ly6G^{hi}Ly6C^{int}), monocytes (Ly6G^{lo}Ly6C^{hi}), and macrophages (CD11b^{+}F4/80^{+}) from *S. aureus*-infected skin on day 7. (*E*) Total number of cells ± SEM on days 3 and 7. $^{*}P < 0.05$, $^{‡}P < 0.001$, as calculated by a two-tailed Student's *t* test. n.s., not significant. Data in *B*, *C*, and *E* are a compilation of two independent experiments.

model in IL-17A/F$^{-/-}$ and wt mice, and skin biopsy specimens on day 7 were evaluated for mRNA levels of these host defense peptides. IL-17A/F$^{-/-}$ mice had a significant decrease in mRNA transcript expression of calprotectin (*S100A8*/*S100A9*, $P < 0.05$) and β-defensins (*DEFB3*, $P < 0.05$; *DEFB4*, $P < 0.01$; and *DEFB14*, $P < 0.05$) but not *LCN2*, *CAMP*, *REG3G*, or *SLURP1*, compared with wt mice (Fig. 4*C*). These results indicate that during an *S. aureus* skin infection, IL-17A/F predominantly regulated the expression of calprotectin and mouse β-defensins 3, 4, and 14.

Vγ6^{+}Vγ4^{+} γδ T Cells Clonally Expanded in LNs in Response to *S. aureus* Skin Infection. Since γδ T cells were the major cellular source of IL-17A in the lymph nodes and *S. aureus*-infected skin (Fig. 2),

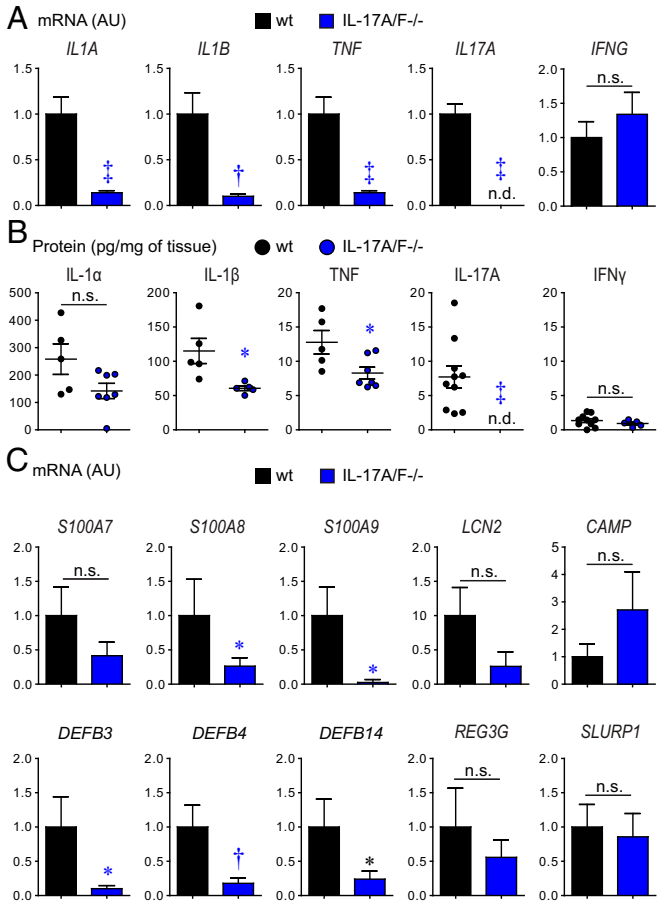

Fig. 4. IL-17A/F regulates cytokine and host defense peptide expression in *S. aureus*-infected skin. *S. aureus* skin infection was performed on IL-17A/F$^{-/-}$ and wt mice and infected skin tissue was harvested on day 7 (n = 5–10 per group). (*A*) Mean mRNA levels of cytokines (arbitrary units; AU) ± SEM. (*B*) Mean protein levels (pg/mg of tissue) ± SEM. (*C*) Mean levels of host defense peptides (AU) ± SEM. $^{*}P < 0.05$, $^{\dagger}P < 0.01$, $^{\ddagger}P < 0.001$, as calculated by a two-tailed Student's t test. n.d., not detected; n.s., not significant. Data are representative of two independent experiments.

we set out to determine if there was clonotypic expansion of γδ T cells (in comparison with αβ T cells) in response to the *S. aureus* skin infection (Fig. 5). TCR nucleotide (nt) sequences encoding complementarity-determining region 3 (CDR3) amino acid sequences were mined from RNA-sequencing (RNA-seq) datasets of day 0 (naïve) and day 28 harvested wt lymph nodes following *S. aureus* skin infection. Results are reported here following International ImMunoGeneTics (IMGT) (http://www.imgt.org/) nomenclature (Fig. 5*A*). The lymph nodes of naïve wt mice had diverse αβ and γδ T cell repertoires with no expanded "public" (present in multiple mice) clones, although unexpanded *TRG*, *TRD*, *TRA*, or *TRB* clones were present in multiple animals (Fig. 5*A*). However, in response to the *S. aureus* skin infection (i.e., day 28), in all wt mice there was a single "top" (dominant) *TRGV6* CDR3-encoding nt sequence that comprised 21% of all *TRG* CDR3-encoding nt sequences, with concomitant expansion of a single top *TRDV4* CDR3-encoding nt sequence that comprised 30% of all *TRD* CDR3-encoding nt sequences (Fig. 5*A*, Table 1, and *SI Appendix*, Tables S1 and S2). This expanded *TRGV6* nt sequence encodes the amino acid sequence CACWDSSGFHKVF, which in this case likely pairs with the expanded *TRD4*-encoded receptor CGSDIGGSSWDTRQMFF. These TCR chains are identical to those expressed by the previously described invariant Vγ6^{+}Vδ4^{+} T cells (previously referred to as Vγ6^{+}Vδ1^{+} T cells according to prior nomenclature) (46), which are resident in the female reproductive tract, lung, and peritoneum and have been shown to preferentially expand in a wide variety of inflammatory settings (47, 48). Interestingly, and as

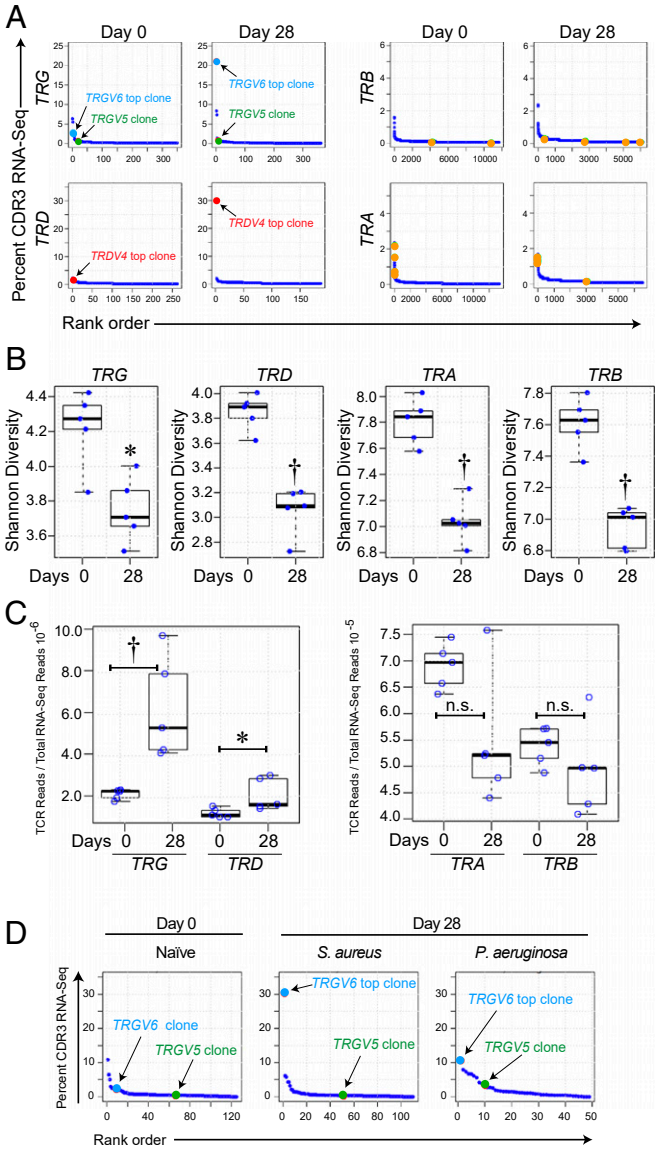

Fig. 5. Clonotypic T cell expansion in lymph nodes in response to *S. aureus* skin infection. TCR complementarity-determining region 3 sequences were mined from an RNA-seq dataset of skin-draining lymph nodes harvested from wt mice on days 0 (naïve) and 28 after *S. aureus* skin infection (n = 5 mice per group) (25). (*A*) Pooled results from all lymph node samples presented as the CDR3 nucleotide sequence rank (x axis) versus the percentage of the total *TRG*, *TRD*, *TRA*, and *TRB* CDR3-encoding nt reads occupied for each particular CDR3 nt sequence (y axis). Dark blue dots indicate each of the different CDR3-encoding nt reads. Light blue dots and red dots indicate top (dominantly expanded) *TRGV6*- and top *TRDV4*-encoding CDR3 nt sequence on day 28 lymph nodes, respectively. Green dots indicate *TRGV5*-encoding CDR3 nt sequence that encodes the exact same amino acid sequence as the top *TRGV6*-encoding CDR3 nt sequence and is expressed by DETCs. Orange dots indicate public (found in all samples) *TRA*- and *TRB*-encoded CDR3 nt sequences. (*B*) Shannon diversity index ± SEM (boxplot: 95% confidence interval). (*C*) Proportion of *TRG*, *TRD*, *TRA*, or *TRB* CDR3-encoding nt reads of total RNA-seq reads ± SEM (boxplot: 95% confidence interval). (*D*) RNA-seq was performed for TCR CDR3 sequences of skin-draining lymph nodes harvested from wt mice on days 0 (naïve) and 28 after *S. aureus* or *P. aeruginosa* skin infection (n = 6 mice per group) (86); data are reported as in *A*. $^{*}P < 0.05$, $^{\dagger}P < 0.01$, as calculated by a Wilcoxon rank-sum test. n.s., not significant.

has been previously noted, the expanded *TRGV6* CDR3 sequence CACWDSSGFHKVF has the exact same CDR3 amino acid sequence as the *TRGV5*-encoding CDR3 sequence expressed by the dendritic epidermal T cells (DETCs), which are $V\gamma5^+V\delta4^+$ γδ T cells that normally reside in mouse epidermis (previously referred to as $V\gamma5^+V\delta1^+$ T cells according to prior nomenclature) (49–51). Therefore, the lymph node RNA-seq dataset was also mined for the *TRGV5* nt sequence of DETCs. Remarkably, even though the canonical *TRGV5* nt sequence encoded the exact same CDR3 amino acid sequence (CACWDSSGFHKVF) as the *S. aureus*-expanded *TRGV6*, there was no expansion of this canonical *TRGV5* nt sequence in response to the *S. aureus* skin infection, as the percentage of *TRGV5* CACWDSSGFHKVF-encoding sequences was similar in wt and day 28 *S. aureus*-infected mice (0.7 and 0.9%, respectively) (Fig. 5*A* and Table 1). Thus, although CACWDSSGFHKVF can be encoded by either *TRGV5* or *TRGV6*, only the *TRGV6*-encoded sequences expand in response to *S. aureus*. There were also public CDR3-encoding *TRA* and *TRB* nt sequences that were present at low frequencies in the lymph nodes of naïve mice (i.e., below 2.5% of the total respective CDR3-encoding nt sequences) (Fig. 5*A*). However, these sequences did not expand following the *S. aureus* skin infection on day 28. Moreover, on day 28, there were no public *TRA* and *TRB* CDR3-encoding nt sequence expansions that were greater than 2% of the total respective *TRA* and *TRB* CDR3-encoding nt sequences in response to the *S. aureus* skin infection.

To determine whether there were similar expansions of the specific *TRGV6* and *TRDV4* nt sequences in *S. aureus*-infected wt mouse skin, we mined the RNA-seq dataset of Brady et al. (52), which included *S. aureus*-infected skin of wt mice on days 0 and 7 (Table 1). This revealed that the same *TRGV6* nt sequence encoding the Vγ6 CDR3 amino acid sequence CACWDSSGFHKVF that expanded in the lymph nodes also expanded in the *S. aureus*-infected skin from 0% (day 0) to 4.6% (day 7). In addition, the same *TRD4* nt sequence encoding the Vδ4 CDR3 amino acid sequence CGSDIGGSSWDTRQMFF that expanded in the lymph nodes also expanded in the *S. aureus*-infected skin from 3.8% (day 0) to 10.9% (day 7). Interestingly, the percentage of the *TRGV5* nt sequence encoding the same CDR3 amino acid sequence as the TCR Vγ6 CDR3 amino acid sequence CACWDSSGFHKVF decreased in the *S. aureus*-infected skin from 15.7% (day 0) to 6.9% (day 7) (Table 1), which was likely in part due to the increased total *TRG* reads caused by the expansion in the clonotypic *TRGV6* nt sequence. Importantly, the *S. aureus*-responsive *TRGV6* clones that expanded in the lymph nodes were undetectable in naïve mouse skin, at the depth of sequencing performed. This supports the data in Figs. 1 and 2, which demonstrate that the immune protection is mediated by T cells that trafficked from the lymph nodes to the *S. aureus*-infected skin.

Next, the diversity of *TRG*, *TRD*, *TRA*, and *TRB* CDR3-encoding nt sequences was then evaluated by calculating their Shannon diversity indices, which demonstrated a statistically significant decrease in the diversity of all of the total respective CDR3-encoding nt sequences in response to the *S. aureus* skin infection on day 28, compared with naïve mice (Fig. 5*B*). These data indicate that the skin-draining αβ T cell repertoire was also altered by *S. aureus* skin infection, although there were no public αβ T cell clonal expansions. Importantly, there are relatively fewer *TRG*- and *TRD*-mapping reads in the skin-draining lymph nodes compared with *TRA*- and *TRB*-mapping reads; however, the proportional increase of *TRG* and *TRD* sequences (respective to total RNA-seq reads) was greater following *S. aureus* skin infection (Fig. 5*C*). This is strong evidence to support the importance of the γδ T cell clonal expansion in the *S. aureus*-induced immune response.

The Clonotypic T Cell Expansion Was More Specific to *S. aureus* Skin Infection. To determine whether the clonotypic *TRGV6* expansion was specific to *S. aureus*, we evaluated whether a similar expansion occurred in response to a gram-negative skin infection with *Pseudomonas aeruginosa*. *P. aeruginosa* induced skin lesions that were smaller than those of *S. aureus* ($P < 0.001$) (*SI Appendix*, Fig. S4 *A* and *B*). However, the in vivo BLI signals of *P. aeruginosa* and *S. aureus* peaked to a similar level on day 1 (*SI Appendix*, Fig. S4 *C* and *D*). *P. aeruginosa* signals then decreased more rapidly than those of *S. aureus* ($P < 0.001$). On day 28, the lymph nodes from the *S. aureus*- and *P. aeruginosa*-infected mice as well as naïve wt mice were harvested, RNA-seq was performed, and TCR nt sequences encoding CDR3 amino acid sequences were mined as in Fig. 5*A*. From these sequences, the percentage of *TRGV6* and *TRGV5* sequences encoding the same clonotypic CDR3 amino acid sequence (CACWDSSGFHKVF) was determined (Fig. 5*D*). In day 0 (naïve) mice, the clonotypic *TRGV6* and *TRGV5* CDR3-encoding nt sequences represented 2.3 and 0.43% of all *TRG* CDR3-encoding nt sequences, respectively. Similar to Fig. 5*A*, in response to *S. aureus*, the clonotypic *TRGV6* sequence markedly expanded 13.3-fold to 30.3% of all *TRG* CDR3-encoding nt sequences, whereas *TRGV5* had no expansion (i.e., 0.37%). In contrast, in response to *P. aeruginosa*, both clonotypic *TRGV6* and *TRGV5* modestly increased to 10.6 and 3.4%, respectively, of all *TRG* CDR3-encoding nt sequences. Thus, following *S. aureus* skin infection, the ratio of the clonotypic *TRGV6* nt sequence to the clonotypic *TRGV5* nt sequence in the skin-draining lymph nodes was 81.9 compared with 3.1 following *P. aeruginosa* skin infection. The latter was similar to the ratio observed in naïve animals (5.3). Taken together, the *P. aeruginosa* skin infection had less specificity, as there was a modest increase in both clonotypic *TRGV6* and *TRGV5* CDR3-encoding nt sequences, whereas the *S. aureus* skin infection induced a specific dominant expansion of only the clonotypic *TRGV6* CDR3-encoding nt sequences.

$V\gamma6^+$ T Cells Are the Most Abundant γδ T Cell Subset in Lymph Nodes. Flow cytometry was used to confirm the RNA-seq data, which indicated a marked expansion of a clonotypic population of $V\gamma6^+V\delta4^+$ γδ T cells. This confirmation is important, because the canonical *TRGV6* and *TRGV5* nt sequences are known to pair with the canonical *TRD4* sequence to encode the same CDR3 amino

Table 1. *TRG* nt sequence alignments

Gene	V	J	CDR3 nt sequence	CDR3 amino acid sequence	Percentage of all CDR3 nt sequences			
					LN day 0	LN day 28	Skin day 0*	Skin day 7*
TRG	*V6*	*J1*	tgtgcatgctgggatagctcaggttttcacaaggtattt	CACWDSSGFHKVF	2.8	21.1	0	4.6
TRG	*V5*	*J1*	tgtgcctgctgggatagctcaggttttcacaaggtattt	CACWDSSGFHKVF	0.7	0.9	15.7	6.9
TRD	*V4*	*J2*	tgtgggtcagatatcggagggagctcctgggacacccgacagatgtttttt	CGSDIGGSSWDTRQMFF	1.6	30.0	3.8	10.9

TRGV6, TRGV5, and *TRDV4 CDR3* nucleotide sequences, gene sequence alignments (underlining indicates nucleotide differences), and respective encoded CDR3 amino acid sequences of the different clonotypes from the *TRG6, TRG5*, and *TRD4 CDR3* reads in Fig. 5*A* and Brady et al. (52). The percentage of each of the specific *TRGV6*, *TRGV5*, or *TRDV4 CDR3* nt sequences of the total number of reads of all respective *TRGV6*, *TRGV5*, or *TRDV4 CDR3* nt sequences is shown for lymph node (LN) specimens from days 0 (naïve) and 28 as well as for skin specimens of *S. aureus*-infected skin from days 0 and 7 from Brady et al. (52). *Brady et al. (52).

acid sequence of Vγ6$^+$Vδ4$^+$ γδ T cells and DETCs, respectively; however, only *TRGV6* and *TRDV4* but not *TRGV5* CDR3-encoding nt sequences expanded. Skin-draining lymph nodes were obtained from wt mice on 0 (naïve), 7, and 28 d following the *S. aureus* skin infection, and the total numbers of Vγ6$^+$ cells, Vγ5$^+$ cells, and a combined group (denoted Vγ1247$^+$) that utilize alternative mouse Vγ chains (i.e., Vγ1, Vγ2, Vγ4, and Vγ7) were determined by flow cytometry [Fig. 6*A*; Vγ3 was not assessed because it is a pseudogene in many mouse strains and, although it might theoretically be functional in C57BL/6 mice, it is so rare it can be disregarded (53, 54)]. The flow cytometry gating strategy first involved gating on live cells, followed by gating on CD3$^+$ TCRγδ$^+$ T cells. Since there is no specific mAb for Vγ6$^+$ cells, γδ T cells were labeled with a mAb against Vγ5 (*y* axis, Fig. 6*A*; clone F536) versus γδ T cells labeled with a combination of mAbs specific for virtually all of the other Vγ chains except Vγ6 (Vγ1 and Vγ2, clone 4B2.9; Vγ4, clone UC3; and Vγ7, clone GL1.7) (*x* axis, Fig. 6*A*). Vγ6$^+$ cells had significantly increased numbers (which steadily increased from day 0 to day 28), compared with either the Vγ1247$^+$ cells (which peaked on day 7 but the numbers were ∼55–80% lower than the Vγ6$^+$ cells) or Vγ5$^+$ cells (which were barely detectable) (Fig. 6*B*). After ex vivo PMA/ionomycin stimulation, there were also significantly increased numbers of Vγ6$^+$IL-17A$^+$, Vγ6$^+$IL-22$^+$, Vγ6$^+$TNF$^+$, and Vγ6$^+$IL-22$^+$ cells (which all peaked on day 7, except for Vγ6$^+$TNF$^+$ cells that steadily increased and peaked on day 28), compared with either the Vγ1247$^+$ cells or Vγ5$^+$ cells (which were barely detectable) (Fig. 6 *C* and *D*). These data confirm that of the γδ T cell subsets present in the skin-draining lymph nodes, Vγ6$^+$ cells represented the greatest number and the most abundant source of IL-17A as well as IL-22, TNF, and IFNγ after ex vivo stimulation. Further, there were barely detectable numbers of Vγ5$^+$ cells in the lymph nodes at all time points evaluated, corroborating the RNA-seq data indicating that Vγ6$^+$ cells rather than Vγ5$^+$ cells were the γδ T cells that expanded in response to the *S. aureus* skin infection.

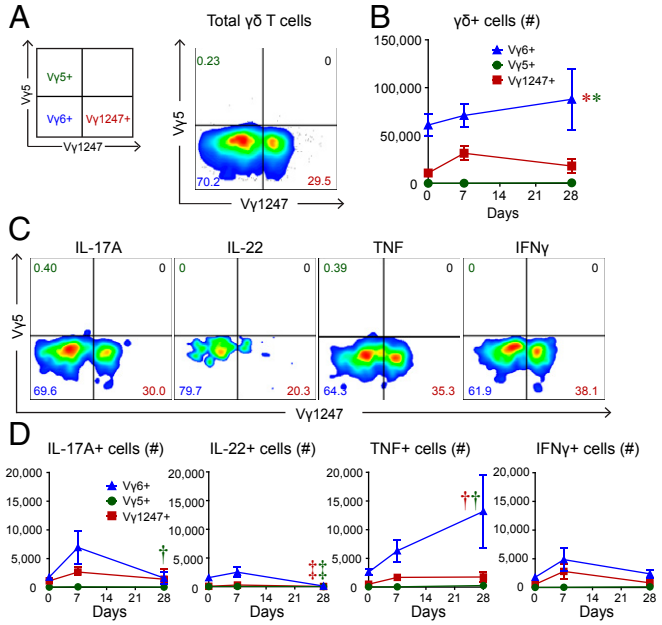

Fig. 6. γδ T cell subsets that expand in response to *S. aureus* skin infection. Skin-draining lymph nodes were harvested from wt mice on days 0 (naïve), 7, and 28 after *S. aureus* skin infection and flow cytometry was performed (n = 5 mice). (*A*) Representative flow plot of γδ T cells (first gated on live cells, then CD3$^+$ and TCRγδ$^+$ cells) from day 7 labeled with mAbs against a combined group of Vγ1, Vγ2, Vγ4, and Vγ7 (i.e., Vγ1247$^+$) (*x* axis) versus a mAb against Vγ5 (i.e., Vγ5$^+$) (*y* axis). Vγ6$^+$ γδ T cells are unlabeled (i.e., Vγ1247$^-$ Vγ5$^-$) (*Left Lower*). (*B*) Total number of cells ± SEM. (*C*) Representative flow plots of IL-17A–, IL-22–, TNF-, and IFNγ-producing Vγ1247$^+$, Vγ5$^+$, and Vγ6$^+$ γδ T cells. (*D*) Total number of cells ± SEM. *$P < 0.05$, †$P < 0.01$, ‡$P < 0.001$, as measured by a two-way ANOVA. Data are representative of two independent experiments.

Discussion

T cells and their cytokine responses have been implicated in host defense against *S. aureus* infections, but whether a predominant T cell subset can mediate protection is not entirely clear. In the present study, we employed a mouse model of *S. aureus* skin infection and found that recruited γδ T cells from lymph nodes to the *S. aureus*-infected skin were critical in mediating IL-17 immune responses, including induction of neutrophil recruitment, proinflammatory cytokines, and host defense peptides. Moreover, the primary T cell source of IL-17 was from a population of clonotypic Vγ6$^+$Vδ4$^+$ γδ T cells expressing a single TCR CDR3 amino acid sequence (generated from canonical *TRGV6* and *TRDV4* nt sequences). Taken together, the findings provide several new and important insights into the role and mechanisms of γδ T cells and ensuing IL-17 responses in host defense and resolution of *S. aureus* skin infections.

First, using an IL-17A/F dual-color reporter mouse strain, we determined that recruited rather than skin-resident T cells were required to mediate host defense against the *S. aureus* skin infection. These results are consistent with the increasing role of IL-17A/F–producing γδ T cells that are rapidly recruited by trafficking through the bloodstream to sites of infection and inflammation in the skin (32, 55–59), including to an *S. aureus* i.p. infection (60). Consistent with these data, flow cytometry revealed that γδ T cells primarily produced IL-17A in the skin-draining lymph nodes and in the *S. aureus*-infected skin to a much greater extent than CD4$^+$ T cells (i.e., Th17 cells), CD8$^+$ T cells, ILC3s, NK cells, or myeloid cells (Fig. 2 *E* and *F*). The trafficking of the γδ T cells to the skin was crucial for host defense, because naïve mouse skin (day 0) had virtually undetectable numbers of IL-17–producing γδ T cells (Fig. 2*D*), and provides an explanation for the impaired host defense in mice treated with FTY720 (Fig. 1 *A* and *B*). Of note, the impairments in lesion size and bacteria burden in FTY720-treated mice occurred earlier (beginning on day 1) compared with those of IL-17A/F$^{-/-}$ mice (beginning on day 3). This difference was likely due to effects of FTY720 other than lymphocyte egress from lymph nodes [reviewed elsewhere (61)], including monocyte egress from the bone marrow or neutrophil recruitment to the skin that might have contributed to host defense against *S. aureus* (62, 63). It should also be mentioned that we found varying expression of IL-17A$^+$, IL-17F$^+$, and IL-17A/F$^+$ γδ and CD4$^+$ T cells from lymph nodes and *S. aureus*-infected skin by flow cytometry (Fig. 2) and γδ and CD4$^+$ T cells from lymph nodes of IL-17A/F dual-color reporter mouse strain in vitro after Th17/IL-17 polarizing conditions (*SI Appendix*, Fig. S1). These findings are consistent with single-cell sequencing of IL-17–producing γδ T cells and Th17 cells (64, 65) and prior results using IL-17 reporter mice created by other groups [e.g., *Il17a*^{Cre}*R26R*^{eYFP} (66), IL-17F-Cre^{EYFP} (67), IL-17F reporter mice (*Il17f*$^{Thy1.1/Thy1.1}$) (68), and Smart-17A mice (surface marker for transcription-17A mice) (69)], which indicate that IL-17A and IL-17F are often coexpressed and can be differentially induced. In particular, differential expression of IL-17A versus IL-17F can be induced by the activity of certain transcription factors such as RORα versus RORγ (70), interleukin-2–inducible T cell kinase (Itk) (71), and STAT3 versus STAT5 (72).

Second, we found that IL-17A and IL-17F had compensatory and redundant roles in host defense during an *S. aureus* skin infection, which is consistent with prior reports in which IL-17A and IL-17F had redundant roles against a mucocutaneous *S. aureus* infection and an adenovirus liver infection (12, 35), and differ from other studies that found differential roles for IL-17A and IL-17F during *S. aureus* pneumonia, contact hypersensitivity, autoimmune encephalomyelitis, arthritis, and chemically induced colitis (12, 36,

37). We also found that γδ T cells primarily produced IL-17A in the *S. aureus*-infected skin (Fig. 2*D*), indicating that γδ T cell-derived IL-17A was critical in orchestrating numerous important cutaneous host defense mechanisms against the *S. aureus* skin infection, including inducing neutrophil recruitment, proinflammatory cytokine production (IL-1α, IL-1β, and TNF but not IFNγ), and host defense peptide production (calprotectin and β-defensins mBD3, mBD4, and mBD14 but not psoriasin, cramp, Reg3γ, or Slurp1).

Most importantly, mining of RNA-seq datasets of skin-draining lymph nodes and infected skin in response to an *S. aureus* skin infection (25, 52) provided new findings that add to the accepted views of mouse γδ T cells. During development, the initial mouse γδ T cells generated in the thymus have canonical TCRs with invariant γ- and δ-chains (46, 51). These invariant γδ T cells disseminate to specific anatomical sites based on the TCR γ-chain they express and are found resident in the female reproductive tract, lung, and peritoneum. They have also been shown to preferentially expand in a wide variety of inflammatory settings (47, 48). Indeed, invariant $V\gamma6^+V\delta4^+$ γδ T cells migrate during development and normally reside in the liver, placenta, kidney, uterus, tongue, and other mucosal sites (47, 48). Additionally, $V\gamma6^+V\delta4^+$ cells were found to normally reside in the dermis of mice (73). However, we found that in response to an *S. aureus* skin infection, invariant $V\gamma6^+V\delta4^+$ γδ T cells expressing the same identical CDR3 amino acid sequence expanded in skin-draining lymph nodes and infected skin of wt mice. In particular, the canonical *TRGV6* and *TRDV4* nt sequences that encoded the invariant CDR3 amino acid sequence of the $V\gamma6^+V\delta4^+$ γδ T cells were found at low frequency in the skin-draining lymph nodes before infection but expanded nearly 10- and 20-fold, respectively, in response to the *S. aureus* skin infection (Table 1). Moreover, the expanded $V\gamma6^+V\delta4^+$ γδ T cells likely trafficked from the lymph nodes to the infected skin to mediate host defense against the *S. aureus* skin infection (0% on day 0 to 4.6% on day 7 of the total *TRG* CDR3 reads in *S. aureus*-infected skin) (Table 1). The canonical *TRDV4* nt sequence is utilized by invariant $V\gamma6^+V\delta4^+$ γδ T cells (47, 48) as well as $V\gamma5^+V\delta4^+$ DETCs that reside in mouse epidermis (49–51). However, we found that both canonical *TRGV6* and *TRGV5* nt sequences were found in the TCR repertoire of lymph nodes in naïve wt mice, but only the *TRGV6* nt sequence expanded in the day 28 lymph nodes and day 7 skin in response to the *S. aureus* skin infection. The mechanism by which $V\gamma6^+V\delta4^+$ γδ T cells and $V\gamma5^+V\delta4^+$ γδ T cells possessing an identical CDR3 amino acid sequence differentially expand in response to the *S. aureus* skin infection is unclear. This differential result could be due to recognition of different antigens. However, the antigen(s) that the CDR3 amino acid sequence of $V\gamma6^+V\delta4^+$ γδ T cells recognizes is unknown (74), and DETCs are thought to recognize a stress-induced self-antigen derived from keratinocytes (51, 75). Nonetheless, since the CDR3 sequences are identical, the difference in expansion could also be due to differential signaling between the TCRs composed of Vγ6 versus Vγ5 chains or expression of costimulatory molecules, transcription factors, and other intrinsic factors between the $V\gamma6^+V\delta4^+$ and $V\gamma5^+V\delta4^+$ γδ T cells. Consistent with the potential differences, an alternative skin infection with *P. aeruginosa* resulted in modest increases of both clonotypic *TRGV6* and *TRGV5* nt sequences, suggesting that the single expansion of $V\gamma6^+V\delta4^+$ T cells might be more specific to *S. aureus* skin infection.

In our recent published report studying IL-1β$^{-/-}$ mice (25), we found that the same CACWDSSGFHKVF CDR3 amino acid sequence expanded in skin-draining lymph nodes; however, it was unknown whether the expansion was encoded for by *TRGV5* or *TRGV6*. At the time, we had presumed that both were expanded because the CACWDSSGFHKVF CDR3 sequence was encoded by both of these TCR gene segments. That manuscript also demonstrated that γδ T cells trafficked from skin-draining lymph nodes to the infected skin during a subsequent *S. aureus* skin infection to produce TNF and IFNγ (but not IL-17A) to mediate host defense (25), which differs from the major role of $V\gamma6^+V\delta4^+$ γδ T cell-derived IL-17A in cutaneous host defense during an initial *S. aureus* skin infection in wt mice described in the present study.

To verify the RNA-seq data by an alternative method, we performed flow cytometry and provide conclusive evidence that $V\gamma6^+$ cells were the most abundant γδ T cell population in the skin-draining lymph nodes that produced IL-17A as well as IL-22, TNF, and IFNγ, which might have also contributed to host defense. The precise mechanisms by which the $V\gamma6^+$ γδ T cells were recruited to the *S. aureus*-infected skin are not entirely clear. However, $V\gamma6^+$IL-17A$^+$ T cells were likely more responsive to chemokine-mediated recruitment, as a significantly higher percentage of these cells expressed CCR2, CCR5, and CCR6 compared with $V\gamma6^+$IL-17A$^-$ T cells (*SI Appendix*, Fig. S5). Our findings are likely broadly applicable to other types of bacterial and fungal infections, as $V\gamma6^+$ γδ T cells have been shown to strongly produce IL-17 and promote host defense at different sites of infection, including i.p. exposure to *S. aureus* (60, 76–78). Although it is unclear whether human γδ T cells (or other human T cell subsets) are the primary source of IL-17 that induces similar protective immunity against *S. aureus* skin infections in humans, the two major populations of human circulating γδ T cells, $V\delta1^+$ and $V\delta2^+$, are increasingly recognized to promote antigen-specific adaptive immunity against different microbial infections (79, 80). The data presented in this study suggest that future investigation into the role of human γδ T cells in host defense against *S. aureus* skin infections might be warranted.

Finally, the current findings add important mechanistic understanding to previous observations of protective immunity in experimental models of *S. aureus* skin infection in mice in which IL-17 responses were shown to play an important role (10, 11, 13–16, 20). Our current results strongly support these prior findings, and now provide specific knowledge that the protective IL-17A–producing T cells identified in these other studies were likely the same specific clonotypic $V\gamma6^+V\delta4^+$ T cells that we identified. This has important implications in host defense against *S. aureus* infections in the skin, and it is unknown whether the same $V\gamma6^+V\delta4^+$ T cells are also involved in protective IL-17 responses against *S. aureus* bloodstream infections or in other organs (17–19), which will be the subject of our future work. Since responses to a vaccine often differ from natural infection, it could also be that antigen-specific αβ T cells might traffic to the skin and provide similar IL-17–mediated protection. Indeed, αβ Th17 cells have been previously associated with vaccine-induced protection against skin and other *S. aureus* infections in mice (18, 20, 81–83). However, as an immune evasion mechanism, *S. aureus* inhibits Th17 and Th1 generation and responses (84), which is consistent with the observed lack of expansion of *TRA* or *TRB CDR3* sequence reads (Fig. 5*A*). Therefore, it could be that the γδ T cell response, which was not inhibited by the *S. aureus* infection, could represent a more effective response to target in future vaccines and immunotherapies.

In summary, clonotypic $V\gamma6^+V\delta4^+$ T cells trafficked from the lymph nodes to the *S. aureus*-infected skin and were critical in inducing IL-17–mediated host defense mechanisms, including neutrophil recruitment and production of proinflammatory cytokines and host defense peptides. These findings increase our mechanistic understanding of T cell responses in immunity to *S. aureus* skin infections and provide a specific clonotypic T cell subset that could be targeted in the development of future vaccines and immunotherapies against *S. aureus* skin infections.

Methods

Bacteria. The bioluminescent *S. aureus* CA-MRSA strain USA300 LAC::*lux* was used in all *S. aureus* experiments and previously generated from the well-described USA300 LAC parent isolate obtained from a CA-MRSA skin infection outbreak in the Los Angeles County Jail (85). USA300 LAC::*lux* possesses a modified *luxABCDE* operon from *Photorhabdus luminescens*, transduced into the bacterial chromosome from the bioluminescent *S. aureus* strain Xen29

(PerkinElmer), and emits bioluminescent signals from live, actively metabolizing bacteria in all states of the *S. aureus* life cycle. The bioluminescent *P. aeruginosa* strain Xen41 (PerkinElmer) was previously generated from the well-characterized PAO1 reference strain.

Preparation of *S. aureus* and *P. aeruginosa* for Skin Inoculation. See *SI Appendix, Methods* for details.

Mice. Six- to 8-wk-old female mice on a C57BL/6 genetic background were used in all experiments. C57BL/6 wt mice were obtained from the Jackson Laboratory. IL-17A/F$^{-/-}$ mice were provided by Yoichiro Iwakura, University of Tokyo, Tokyo, and generated as previously described (12). IL-17A-tdTomato/IL-17F-GFP dual-color reporter mice on a C57BL/6 background were generated as described below.

Generation of IL-17A/F Dual-Color Reporter Mice. A bacterial artificial chromosome was modified to introduce two fluorescent reporter genes into the *Il17* locus, which includes IL-17A and IL-17F. By homologous recombination, the synthesis of the signal peptide of *Il17a/f* in the BAC was disrupted and the *GFP* gene with *polyA* was inserted immediately after the *ATG* start site of *Il17f*, replacing exon 1, while the *tdTomato* gene with *poly(A)* was inserted immediately after the *ATG* start site of *Il17a*. BAC end-sequencing and DNA-fingerprinting results showed that there is no rearrangement and deletion of the BAC construct with the reporter gene. Mice on a C57BL/6 background were generated that harbor the BAC construct. Description of the methods for validation of the reporter mouse strain can be found in *SI Appendix, Methods*.

Mouse Model of *S. aureus* Skin Infection and Lesion Size Quantification. All experiments were approved by the Johns Hopkins Animal Care and Use Committee. This mouse model of intradermal *S. aureus* infection was performed as previously described (11, 25, 29–31). Briefly, mice were anesthetized (2% isoflurane), and the dorsal backs were shaved and injected intradermally with 3×10^7 CFUs/100 μL PBS of CA-MRSA strain USA300 LAC::*lux* using a 29-gauge insulin syringe. In some experiments, IL-17A/F dual-color reporter mice were injected intraperitoneally with FTY720 (Sigma-Aldrich), 1 mg/kg in 100 μL sterile water on days −1, 0, and 1, and every other day thereafter until the experiment was arbitrarily ended on day 14, according to previously described methods (25, 32). In some experiments, wt mice were treated intraperitoneally with anti–IL-17A mAb (clone 17F3; BioXCell), anti–IL-17F mAb (clone MM17F8F5.1A9; BioXCell), or combined anti–IL-17A and anti–IL-17F mAb each on days −1 and 0 (200 μg/100 μL) and every other day thereafter (100 μg/100 μL) until the experiment was arbitrarily ended on day 14, modified from previously described methods (10). In other experiments, IL-17A/F$^{-/-}$ mice were treated with recombinant IL-17A or rIL-17F (1,000 ng) that was included with the i.d. bacterial inoculum, modified from previously described methods (11). Total lesion size (cm^2) was measured by analyzing digital photographs using ImageJ (https://imagej.nih.gov/ij/) and a millimeter ruler as a reference.

Quantification of *S. aureus* by in Vivo BLI and ex Vivo CFUs. Mice were anesthetized via inhalation of isoflurane (2%), and in vivo BLI was performed using a Lumina III IVIS (PerkinElmer); total flux (photons/s) was measured within a 1×10^3-pixel circular region of interest using Living Image software (PerkinElmer) (limit of detection, 2×10^4 photons/s). The in vivo bioluminescent signals of USA300 LAC::*lux* closely approximate the ex vivo CFUs from homogenized skin obtained at different time points after infection (correlation coefficient, $R^2 = 0.9996$) (33). Ex vivo CFUs were enumerated from overnight cultures of serially diluted 10-mm lesional skin punch biopsy specimens homogenized at 4 °C (Pro200 Series homogenizer; Pro Scientific).

Mouse Model of *P. aeruginosa* Skin Infection. See *SI Appendix, Methods* for details.

Histology and Immunofluorescence Microscopy. See *SI Appendix, Methods* for details.

Flow Cytometry. For skin specimens, 10-mm skin punch biopsies were minced and placed in 3 mL RPMI containing 100 μg/mL DNaseI (Sigma-Aldrich) and 1.67 Wunsch units/mL Liberase TL (Roche). Skin was digested for 1 h at 37 °C and shaken at 140 rpm. For skin and lymph node specimens, single cells were isolated by manually pushing grinded skin or lymph nodes with a 3-mL syringe plunger through a 40-μm cell strainer and the cells were then washed in RPMI. For additional flow cytometry methods, see *SI Appendix, Methods*.

RNA Extraction and mRNA Quantification for Gene Expression Arrays. See *SI Appendix, Methods* for details.

Cytokine Protein Levels. Protein levels (pg/mg tissue weight) of IL-1α, IL-1β, TNF, IL-17A, and IFNγ were measured from homogenized 10-mm skin punch biopsies collected on days 0 and 7 following *S. aureus* skin infection by ELISA according to the manufacturer's recommendations (R&D Systems).

In Vivo Fluorescence Imaging of IL-17A/F–Producing Cells. Mice were anesthetized with inhalation isoflurane, and in vivo FLI was performed sequentially after in vivo BLI using a Lumina III IVIS (PerkinElmer). tdTomato fluorescence was measured using excitation 554 nm, emission 581 nm, and exposure time 0.5 s. GFP fluorescence was measured using excitation 488 nm, emission 507 nm, and exposure time 0.5 s. Data are presented on a color scale overlaid on a grayscale photograph of mice and quantified as total radiant efficiency ([photons/s]/[mW/cm^2]) within a circular region of interest using Living Image software (PerkinElmer).

Analysis of Public RNA-Seq Datasets. See *SI Appendix, Methods* and our previously described methods (25).

RNA Isolation, RNA-Seq and Analysis, Amplification of TCR CDR3, TCR Library Preparation, and TCR Library Sequencing and Analysis. See *SI Appendix, Methods*, ref. 86, and our previously described methods (25).

Statistical Analysis. For all data except the RNA-seq analyses, data for single comparisons were compared using a two-tailed Student's *t* test and data for multiple comparisons were compared using a two-way ANOVA using Prism software (GraphPad). For the RNA-seq datasets, Shannon diversity indices were calculated using the "vegan" R package (87), and the Wilcoxon rank-sum test was used for all between-group comparisons and all pairwise comparisons. Values of $P < 0.05$ for all statistical comparisons were considered to be statistically significant.

ACKNOWLEDGMENTS. We thank Tammy Kielian (University of Nebraska) for providing the USA300 LAC::*lux* strain, Yoichiro Iwakura (University of Tokyo) for providing the IL-17A/F$^{-/-}$ mice, and AstraZeneca for providing the anti-LTA antibody. This work was supported by grants from the National Institute of Arthritis and Musculoskeletal and Skin Diseases (R01AR069502 and R01AR073665), grants from the National Institute of Allergy and Infectious Diseases (R21AI126896 to L.S.M.; U01AI124319 and R33AI111661 to M.R.Y.; and R01AI129302 to S.I.S.), a grant from the National Institute of Neurological Disorders and Stroke (R01NS054791 to X.D.), and federal funds from the National Cancer Institute under Contract HHSN261200800001E (to S.K.D.) and a grant from the Office of the NIH Director (1DP2OD008752 to E.M.) from the National Institutes of Health. The content of this publication does not necessarily reflect the views or policies of the Department of Health and Human Services, nor does mention of trade names, commercial products, or organizations imply endorsement by the US Government.

1. Miller LS, Cho JS (2011) Immunity against *Staphylococcus aureus* cutaneous infections. *Nat Rev Immunol* 11:505–518.
2. DeLeo FR, Otto M, Kreiswirth BN, Chambers HF (2010) Community-associated meticillin-resistant *Staphylococcus aureus*. *Lancet* 375:1557–1568.
3. Tong SY, Davis JS, Eichenberger E, Holland TL, Fowler VG, Jr (2015) *Staphylococcus aureus* infections: Epidemiology, pathophysiology, clinical manifestations, and management. *Clin Microbiol Rev* 28:603–661.
4. Missiakas D, Schneewind O (2016) *Staphylococcus aureus* vaccines: Deviating from the carol. *J Exp Med* 213:1645–1653.
5. Fowler VG, et al. (2013) Effect of an investigational vaccine for preventing *Staphylococcus aureus* infections after cardiothoracic surgery: A randomized trial. *JAMA* 309:1368–1378.
6. Ma CS, et al. (2008) Deficiency of Th17 cells in hyper IgE syndrome due to mutations in STAT3. *J Exp Med* 205:1551–1557.
7. Milner JD, et al. (2008) Impaired T(H)17 cell differentiation in subjects with autosomal dominant hyper-IgE syndrome. *Nature* 452:773–776.
8. Puel A, et al. (2011) Chronic mucocutaneous candidiasis in humans with inborn errors of interleukin-17 immunity. *Science* 332:65–68.
9. Renner ED, et al. (2008) Novel signal transducer and activator of transcription 3 (STAT3) mutations, reduced T(H)17 cell numbers, and variably defective STAT3 phosphorylation in hyper-IgE syndrome. *J Allergy Clin Immunol* 122:181–187.
10. Chan LC, et al. (2015) Nonredundant roles of interleukin-17A (IL-17A) and IL-22 in murine host defense against cutaneous and hematogenous infection due to methicillin-resistant *Staphylococcus aureus*. *Infect Immun* 83:4427–4437.
11. Cho JS, et al. (2010) IL-17 is essential for host defense against cutaneous *Staphylococcus aureus* infection in mice. *J Clin Invest* 120:1762–1773.
12. Ishigame H, et al. (2009) Differential roles of interleukin-17A and -17F in host defense against mucoepithelial bacterial infection and allergic responses. *Immunity* 30:108–119.
13. Maher BM, et al. (2013) Nlrp-3-driven interleukin 17 production by γδT cells controls infection outcomes during *Staphylococcus aureus* surgical site infection. *Infect Immun* 81:4478–4489.

14. Montgomery CP, et al. (2014) Protective immunity against recurrent *Staphylococcus aureus* skin infection requires antibody and interleukin-17A. *Infect Immun* 82:2125–2134.
15. Myles IA, et al. (2013) Signaling via the IL-20 receptor inhibits cutaneous production of IL-1β and IL-17A to promote infection with methicillin-resistant *Staphylococcus aureus*. *Nat Immunol* 14:804–811.
16. Tkaczyk C, et al. (2013) *Staphylococcus aureus* alpha toxin suppresses effective innate and adaptive immune responses in a murine dermonecrosis model. *PLoS One* 8:e75103.
17. Joshi A, et al. (2012) Immunization with *Staphylococcus aureus* iron regulated surface determinant B (IsdB) confers protection via Th17/IL17 pathway in a murine sepsis model. *Hum Vaccin Immunother* 8:336–346.
18. Lin L, et al. (2009) Th1-Th17 cells mediate protective adaptive immunity against *Staphylococcus aureus* and *Candida albicans* infection in mice. *PLoS Pathog* 5:e1000703.
19. Narita K, et al. (2010) Role of interleukin-17A in cell-mediated protection against *Staphylococcus aureus* infection in mice immunized with the fibrinogen-binding domain of clumping factor A. *Infect Immun* 78:4234–4242.
20. Yeaman MR, et al. (2014) Mechanisms of NDV-3 vaccine efficacy in MRSA skin versus invasive infection. *Proc Natl Acad Sci USA* 111:E5555–E5563.
21. Brown AF, et al. (2015) Memory Th1 cells are protective in invasive *Staphylococcus aureus* infection. *PLoS Pathog* 11:e1005226.
22. McLoughlin RM, Lee JC, Kasper DL, Tzianabos AO (2008) IFN-gamma regulated chemokine production determines the outcome of *Staphylococcus aureus* infection. *J Immunol* 181:1323–1332.
23. Utay NS, et al. (2016) MRSA infections in HIV-infected people are associated with decreased MRSA-specific Th1 immunity. *PLoS Pathog* 12:e1005580.
24. Uebele J, et al. (2017) Antigen delivery to dendritic cells shapes human $CD4^+$ and $CD8^+$ T cell memory responses to *Staphylococcus aureus*. *PLoS Pathog* 13:e1006387.
25. Dillen CA, et al. (2018) Clonally expanded γδ T cells protect against *Staphylococcus aureus* skin reinfection. *J Clin Invest* 128:1026–1042.
26. Malhotra N, et al. (2016) IL-22 derived from gammadelta T cells restricts *Staphylococcus aureus* infection of mechanically injured skin. *J Allergy Clin Immunol* 138:1098–1107.e3.
27. Moriwaki Y, et al. (2015) IL-22/STAT3-induced increases in SLURP1 expression within psoriatic lesions exerts antimicrobial effects against *Staphylococcus aureus*. *PLoS One* 10:e0140750.
28. Mulcahy ME, Leech JM, Renauld JC, Mills KH, McLoughlin RM (2016) Interleukin-22 regulates antimicrobial peptide expression and keratinocyte differentiation to control *Staphylococcus aureus* colonization of the nasal mucosa. *Mucosal Immunol* 9:1429–1441.
29. Miller LS, et al. (2006) MyD88 mediates neutrophil recruitment initiated by IL-1R but not TLR2 activation in immunity against *Staphylococcus aureus*. *Immunity* 24:79–91.
30. Cho JS, et al. (2011) Noninvasive in vivo imaging to evaluate immune responses and antimicrobial therapy against *Staphylococcus aureus* and USA300 MRSA skin infections. *J Invest Dermatol* 131:907–915.
31. Cho JS, et al. (2012) Neutrophil-derived IL-1β is sufficient for abscess formation in immunity against *Staphylococcus aureus* in mice. *PLoS Pathog* 8:e1003047.
32. Ramírez-Valle F, Gray EE, Cyster JG (2015) Inflammation induces dermal $V\gamma4^+$ γδT17 memory-like cells that travel to distant skin and accelerate secondary IL-17–driven responses. *Proc Natl Acad Sci USA* 112:8046–8051.
33. Guo Y, et al. (2013) In vivo bioluminescence imaging to evaluate systemic and topical antibiotics against community-acquired methicillin-resistant *Staphylococcus aureus*-infected skin wounds in mice. *Antimicrob Agents Chemother* 57:855–863.
34. Taylor PR, et al. (2014) Activation of neutrophils by autocrine IL-17A-IL-17RC interactions during fungal infection is regulated by IL-6, IL-23, RORγt and dectin-2. *Nat Immunol* 15:143–151.
35. Jie Z, et al. (2014) Intrahepatic innate lymphoid cells secrete IL-17A and IL-17F that are crucial for T cell priming in viral infection. *J Immunol* 192:3289–3300.
36. Shibue Y, et al. (2019) Role of interleukin-17 in a murine community-associated methicillin-resistant *Staphylococcus aureus* pneumonia model. *Microbes Infect* 21:33–39.
37. Chen F, et al. (2016) mTOR mediates IL-23 induction of neutrophil IL-17 and IL-22 production. *J Immunol* 196:4390–4399.
38. Archer NK, et al. (2019) Injury, dysbiosis, and filaggrin deficiency drive skin inflammation through keratinocyte IL-1α release. *J Allergy Clin Immunol* 143:1426–1443.e6.
39. Corbin BD, et al. (2008) Metal chelation and inhibition of bacterial growth in tissue abscesses. *Science* 319:962–965.
40. Hinrichsen K, et al. (2008) Mouse beta-defensin-14, an antimicrobial ortholog of human beta-defensin-3. *Antimicrob Agents Chemother* 52:1876–1879.
41. Röhrl J, Yang D, Oppenheim JJ, Hehlgans T (2008) Identification and biological characterization of mouse beta-defensin 14, the orthologue of human beta-defensin 3. *J Biol Chem* 283:5414–5419.
42. Breyne K, Steenbrugge J, Demeyere K, Vanden Berghe T, Meyer E (2017) Preconditioning with lipopolysaccharide or lipoteichoic acid protects against *Staphylococcus aureus* mammary infection in mice. *Front Immunol* 8:833.
43. Braff MH, Zaiou M, Fierer J, Nizet V, Gallo RL (2005) Keratinocyte production of cathelicidin provides direct activity against bacterial skin pathogens. *Infect Immun* 73:6771–6781.
44. Zhang LJ, et al. (2015) Innate immunity. Dermal adipocytes protect against invasive *Staphylococcus aureus* skin infection. *Science* 347:67–71.
45. Choi SM, et al. (2013) Innate Stat3-mediated induction of the antimicrobial protein Reg3γ is required for host defense against MRSA pneumonia. *J Exp Med* 210:551–561.
46. Itohara S, et al. (1990) Homing of a γδ thymocyte subset with homogeneous T-cell receptors to mucosal epithelia. *Nature* 343:754–757.
47. Bonneville M, O'Brien RL, Born WK (2010) Gammadelta T cell effector functions: A blend of innate programming and acquired plasticity. *Nat Rev Immunol* 10:467–478.
48. Muñoz-Ruiz M, Sumaria N, Pennington DJ, Silva-Santos B (2017) Thymic determinants of γδ T cell differentiation. *Trends Immunol* 38:336–344.
49. Asarnow DM, Goodman T, LeFrancois L, Allison JP (1989) Distinct antigen receptor repertoires of two classes of murine epithelium-associated T cells. *Nature* 341:60–62.
50. Asarnow DM, et al. (1988) Limited diversity of γδ antigen receptor genes of Thy-1^+ dendritic epidermal cells. *Cell* 55:837–847.
51. Havran WL, Chien YH, Allison JP (1991) Recognition of self antigens by skin-derived T cells with invariant gamma delta antigen receptors. *Science* 252:1430–1432.
52. Brady RA, Bruno VM, Burns DL (2015) RNA-seq analysis of the host response to *Staphylococcus aureus* skin and soft tissue infection in a mouse model. *PLoS One* 10:e0124877.
53. Hayday AC, et al. (1985) Structure, organization, and somatic rearrangement of T cell gamma genes. *Cell* 40:259–269.
54. Pereira P, et al. (1996) Rearrangement and expression of Vγ1, Vγ2 and Vγ3 TCR γ genes in C57BL/6 mice. *Int Immunol* 8:83–90.
55. Cai Y, et al. (2011) Pivotal role of dermal IL-17-producing γδ T cells in skin inflammation. *Immunity* 35:596–610.
56. Gray EE, Suzuki K, Cyster JG (2011) Cutting edge: Identification of a motile IL-17-producing gammadelta T cell population in the dermis. *J Immunol* 186:6091–6095.
57. Mabuchi T, Takekoshi T, Hwang ST (2011) Epidermal $CCR6^+$ γδ T cells are major producers of IL-22 and IL-17 in a murine model of psoriasiform dermatitis. *J Immunol* 187:5026–5031.
58. Pantelyushin S, et al. (2012) $Ror\gamma t^+$ innate lymphocytes and γδ T cells initiate psoriasiform plaque formation in mice. *J Clin Invest* 122:2252–2256.
59. Sumaria N, et al. (2011) Cutaneous immunosurveillance by self-renewing dermal gammadelta T cells. *J Exp Med* 208:505–518.
60. Murphy AG, et al. (2014) *Staphylococcus aureus* infection of mice expands a population of memory γδ T cells that are protective against subsequent infection. *J Immunol* 192:3697–3708.
61. Cyster JG, Schwab SR (2012) Sphingosine-1-phosphate and lymphocyte egress from lymphoid organs. *Annu Rev Immunol* 30:69–94.
62. Shi C, et al. (2011) Bone marrow mesenchymal stem and progenitor cells induce monocyte emigration in response to circulating Toll-like receptor ligands. *Immunity* 34:590–601.
63. Sun WY, et al. (2016) Topical application of fingolimod perturbs cutaneous inflammation. *J Immunol* 196:3854–3864.
64. Gaublomme JT, et al. (2015) Single-cell genomics unveils critical regulators of Th17 cell pathogenicity. *Cell* 163:1400–1412.
65. Zuberbuehler MK, et al. (2019) The transcription factor c-Maf is essential for the commitment of IL-17-producing γδ T cells. *Nat Immunol* 20:73–85.
66. Hirota K, et al. (2011) Fate mapping of IL-17-producing T cells in inflammatory responses. *Nat Immunol* 12:255–263.
67. Croxford AL, Kurschus FC, Waisman A (2009) Cutting edge: An IL-17F-Cre^{EYFP} reporter mouse allows fate mapping of Th17 cells. *J Immunol* 182:1237–1241.
68. Lee YK, et al. (2009) Late developmental plasticity in the T helper 17 lineage. *Immunity* 30:92–107.
69. Price AE, Reinhardt RL, Liang HE, Locksley RM (2012) Marking and quantifying IL-17A-producing cells in vivo. *PLoS One* 7:e39750.
70. Yang XO, et al. (2008) T helper 17 lineage differentiation is programmed by orphan nuclear receptors RORα and RORγ. *Immunity* 28:29–39.
71. Gomez-Rodriguez J, et al. (2009) Differential expression of interleukin-17A and -17F is coupled to T cell receptor signaling via inducible T cell kinase. *Immunity* 31:587–597.
72. Yang XP, et al. (2011) Opposing regulation of the locus encoding IL-17 through direct, reciprocal actions of STAT3 and STAT5. *Nat Immunol* 12:247–254.
73. Cai Y, et al. (2014) Differential developmental requirement and peripheral regulation for dermal Vγ4 and Vγ6T17 cells in health and inflammation. *Nat Commun* 5:3986.
74. Willcox BE, Willcox CR (2019) γδ TCR ligands: The quest to solve a 500-million-year-old mystery. *Nat Immunol* 20:121–128.
75. Komori HK, et al. (2012) Cutting edge: Dendritic epidermal γδ T cell ligands are rapidly and locally expressed by keratinocytes following cutaneous wounding. *J Immunol* 188:2972–2976.
76. Conti HR, et al. (2014) Oral-resident natural Th17 cells and γδ T cells control opportunistic *Candida albicans* infections. *J Exp Med* 211:2075–2084.
77. Misiak A, Wilk MM, Raverdeau M, Mills KH (2017) IL-17-producing innate and pathogen-specific tissue resident memory γδ T cells expand in the lungs of *Bordetella pertussis*-infected mice. *J Immunol* 198:363–374.
78. Okamoto Yoshida Y, et al. (2010) Essential role of IL-17A in the formation of a mycobacterial infection-induced granuloma in the lung. *J Immunol* 184:4414–4422.
79. Davey MS, et al. (2017) Clonal selection in the human Vδ1 T cell repertoire indicates γδ TCR-dependent adaptive immune surveillance. *Nat Commun* 8:14760.
80. Dimova T, et al. (2015) Effector Vγ9Vδ2 T cells dominate the human fetal γδ T-cell repertoire. *Proc Natl Acad Sci USA* 112:E556–E565.
81. Bagnoli F, et al. (2015) Vaccine composition formulated with a novel TLR7-dependent adjuvant induces high and broad protection against *Staphylococcus aureus*. *Proc Natl Acad Sci USA* 112:3680–3685.
82. Lacey KA, et al. (2017) The *Staphylococcus aureus* cell wall-anchored protein clumping factor A is an important T cell antigen. *Infect Immun* 85:e00549-17.
83. Zhang R, et al. (2018) Mechanisms of fibronectin-binding protein A ($FnBPA_{110-263}$) vaccine efficacy in *Staphylococcus aureus* sepsis versus skin infection. *Clin Immunol* 194:1–8.
84. Sanchez M, et al. (2017) O-acetylation of peptidoglycan limits helper T cell priming and permits *Staphylococcus aureus* reinfection. *Cell Host Microbe* 22:543–551.e4.
85. Thurlow LR, et al. (2011) *Staphylococcus aureus* biofilms prevent macrophage phagocytosis and attenuate inflammation in vivo. *J Immunol* 186:6585–6596.
86. Meerlev AA (2019) Clonal $V\gamma6^+V\delta4^+$ T cells promote IL-17-mediated immunity against *Staphylococcus aureus* skin infection. NCBI Sequence Read Archive. Available at https://www.ncbi.nlm.nih.gov/sra?term=SRP194263. Deposited April 29, 2019.
87. Oksanen J, et al. (2019) vegan: Community Ecology Package. R Package Version 2.5-4. Available at https://cran.r-project.org/web/packages/vegan/index.html. Accessed April 29, 2019.